

This is an Open Access document downloaded from ORCA, Cardiff University's institutional repository: <https://orca.cardiff.ac.uk/id/eprint/113164/>

This is the author's version of a work that was submitted to / accepted for publication.

Citation for final published version:

Connolly, Katherine D. , Wadey, Rebecca M., Mathew, Donna, Johnson, Errin, Rees, D. Aled and James, Philip E.. 2018. Evidence for adipocyte-derived extracellular vesicles in the human circulation. *Endocrinology* 159 (9) , pp. 3259-3267. 10.1210/en.2018-00266

Publishers page: <https://doi.org/10.1210/en.2018-00266>

Please note:

Changes made as a result of publishing processes such as copy-editing, formatting and page numbers may not be reflected in this version. For the definitive version of this publication, please refer to the published source. You are advised to consult the publisher's version if you wish to cite this paper.

This version is being made available in accordance with publisher policies. See <http://orca.cf.ac.uk/policies.html> for usage policies. Copyright and moral rights for publications made available in ORCA are retained by the copyright holders.



# EVIDENCE FOR ADIPOCYTE-DERIVED EXTRACELLULAR VESICLES IN THE HUMAN CIRCULATION

Katherine D. Connolly<sup>1</sup>, Rebecca M. Wadey<sup>1</sup>, Donna Mathew<sup>1,2</sup>, Errin Johnson<sup>3</sup> D Aled Rees<sup>2</sup>, Philip E. James<sup>1\*</sup>

<sup>1</sup>School of Sport and Health Sciences, Cardiff Metropolitan University, Cardiff, UK, CF5 2YB.

<sup>2</sup>Neuroscience and Mental Health Research Institute, School of Medicine, Cardiff University, Cardiff, UK, CF24 4HQ.

<sup>3</sup>Sir William Dunn School of Pathology, University of Oxford, Oxford, UK, OX1 3RE.

Short title: **CIRCULATING ADIPOCYTE EXTRACELLULAR VESICLES**

Keywords: Extracellular vesicles; adipocytes; adipocyte-derived extracellular vesicles; circulating biomarkers.

*\*Corresponding author and to whom reprint requests should be addressed:*

PE James, School of Sport and Health Sciences, Cardiff Metropolitan University, Western Avenue, Cardiff, CF5 2YB. Phone: +44 (0) 292041 7129, E-mail: [pjames@cardiffmet.ac.uk](mailto:pjames@cardiffmet.ac.uk)

## Sources of Funding

This work was supported by the Ewan Maclean Scholarship fund (Cardiff University), the British Heart Foundation and Cardiff Metropolitan University.

## Disclosures

The authors have nothing to disclose.

## **Abstract**

Adipocyte-derived extracellular vesicles (EVs) may serve as novel endocrine mediators of adipose tissue and impact upon vascular health. However, it is unclear whether adipocyte-derived EVs are present in the human circulation. Therefore, the purpose of this study was to seek evidence for the presence of adipocyte-derived EVs in circulating plasma. Size exclusion chromatography of platelet-free plasma identified fractions 5-10 as containing EVs by a peak in particle concentration, which corresponded with the presence of EV and adipocyte proteins. Pooling fractions 5-10 and subjecting to ultracentrifugation yielded a plasma EV sample, as verified by transmission electron microscopy (TEM) showing EV structures and Western blotting for EV (e.g. CD9 and Alix) and adipocyte markers. Magnetic beads and a solid phase assay were used to deplete the EV sample of the four major families of circulating EVs: platelet-, leukocyte-, endothelial- and erythrocyte-derived EVs. Post-depletion samples from both techniques contained EV structures as visualized by TEM, as well as CD9, Alix and classic adipocyte proteins. Post-depletion samples also contained a range of other adipocyte proteins from an adipokine array. Adipocyte proteins and adipokines are expressed in optimally processed plasma EV samples, suggesting that adipocyte-derived EVs are secreted into the human circulation.

## **Précis**

Optimally isolated, human plasma-derived extracellular vesicles were found to contain multiple adipocyte markers, even after the depletion of major circulating extracellular vesicle populations.

## Introduction

The endocrine functions of adipose tissue have largely been attributed to adipokines; an array of soluble bioactive molecules secreted from adipocytes such as adiponectin and fatty acid binding protein (FABP)-4<sup>1</sup>. Dysregulation of adipokine secretion is associated with obesity-related cardiovascular disease, insulin resistance, and type 2 diabetes<sup>2</sup>. Adiponectin, peroxisome proliferator-activated receptor (PPAR)- $\gamma$ , FABP4 and Perilipin have been detected within adipocyte-derived extracellular vesicles (EVs) *in vitro*<sup>3–12</sup> indicating an additional method for endocrine signalling from adipose tissue. Dysfunctional adipocytes in obese adipose tissue may release an altered complement of EVs, which in addition to dysregulated adipokine secretion, help to promote the cardiovascular complications associated with obesity. Therefore, there is a need for comprehensive evidence for the existence of adipocyte-derived EVs *in vivo* to explore their potential as novel circulating biomarkers of adipocytes *in vivo*.

EVs are heterogeneous submicron vesicles released from almost all cells in response to cellular stress, activation or apoptosis. EVs may originate from cytoplasmic multivesicular bodies which fuse with the plasma membrane to release vesicles typically <120 nm in diameter, often referred to as exosomes. EVs also include microvesicles, which are ~ 100-1000 nm in size and bud directly from the plasma membrane into the extracellular space. Both subclasses of EVs have a biomolecular composition similar to that of the original cell including specific lipids, proteins, and nucleic acids. Recent advances in methodology have enabled standardisation of nomenclature and characterisation of EV populations<sup>13</sup>.

Most studies examining the release of EVs from adipocytes have been conducted *in vitro* using 3T3-L1 cells<sup>3,6–9,11,12</sup>; a murine adipocyte cell line frequently used to model adipocyte functions. Others have also isolated EVs from human adipocytes and adipose tissue extracts<sup>4,5,10</sup>. These studies have demonstrated the functional relevance of adipocyte-derived EVs in the paracrine regulation of adipocyte metabolism<sup>14</sup>, monocyte to macrophage differentiation<sup>4</sup> and regulation of hepatic insulin signaling<sup>5</sup>. Effects on vascular homeostasis have also been shown, including induction of

neovascularization and angiogenesis<sup>15,16</sup>, suggesting that adipocyte-derived EVs may influence vascular health within, and at sites remote to adipose tissue. However, evidence for the presence of adipocyte-derived EVs in the human circulation has not yet been confirmed, since EVs in blood are thought to derive primarily from platelets (with leukocyte-, endothelial- and erythrocyte-derived EVs contributing smaller populations<sup>17–19</sup>), and adipocytes lack a unique marker to readily distinguish them from other cells. Preliminary evidence from flow cytometric analyses showed that EVs contain the adipocyte markers FABP4 and adiponectin in human and mouse plasma<sup>18,20</sup>. However, the use of direct flow cytometry for EV measurements is sub-optimal as the lower limit of detection for many conventional flow cytometers is ~300 nm<sup>21</sup>, resulting in an incomplete assessment of the EV population. Separate studies have also shown that adiponectin, FABP4, Perilipin and PPAR- $\gamma$  were associated with plasma EVs<sup>4,11,22</sup> though in most cases, plasma samples were not processed in accordance with guidelines set out by the International Society for Extracellular Vesicles (ISEV)<sup>13</sup>. This may lead to false positive results from contamination of soluble adipokines present in the larger plasma protein pool.

In light of these uncertainties, we utilized a combination of adipocyte markers and sample processing according to ISEV recommendations to seek evidence for the presence of adipocyte-derived EVs in healthy human plasma.

## Materials and Methods

### *Plasma EV isolation*

Ethical approval for this study was granted by Cardiff Metropolitan University School Research Ethics Committee and informed consent was obtained from each volunteer. Blood was drawn from seven healthy volunteers (3 males, 4 females) using a 19 G needle into 3.2% (w/v) sodium citrate vacutainers and immediately centrifuged (2500 x g, 15 minutes, 21°C) to isolate platelet-poor plasma (PPP). The first 3 mL of blood was discarded in line with recommended guidelines for collection of EVs from blood<sup>23,24</sup>. PPP was then pooled and centrifuged as above to isolate platelet-free plasma (PFP). PFP (1 mL) was then loaded onto Exo-spin™ midi size exclusion columns (Cell Guidance Systems, UK) and 30 x 500 µL fractions were collected. Fractions 5-10 were then pooled and ultracentrifuged (100,000 x g, 1 hour, 4°C) to pellet EVs (hereafter referred to as “pooled EVs”).

### *Nanoparticle Tracking Analysis*

Quantification of EV populations was performed using nanoparticle tracking analysis (NTA) with a NanoSight LM10 instrument configured with a 488 nm laser and a sCMOS camera (Malvern Instruments Ltd, UK). A Harvard Apparatus syringe pump was utilized for EV measurements at a constant flow rate of 20 a.u. Camera shutter speed and gain were maintained at 607 and 15 respectively. Sample videos were recorded for 60 seconds in repetitions of 5 using a capture screen gain of 8-11 and a camera level of 8-10. Samples were processed using a screen gain of 20 and a detection threshold of 4-6. Software version 3.1 (build 3.1.54) was used for capture and analysis. All experiments were performed in a temperature-controlled room at 22°C. Results are presented as particles/mL.

## *Western Blotting*

The protein concentration of individual column fractions (1-30) was determined using a NanoDrop 1000 Spectrophotometer (ThermoFisher Scientific, UK). Samples (8 µg) of fractions 2-28, pooled EVs and post-depletion samples were prepared to 30 µL (neat or diluted with 1X PBS), boiled for 8 minutes on a heat block, centrifuged (12,000 x g, 5 mins, 4°C) and kept on ice before loading onto 4-12% Bis-Tris gels (ThermoFisher Scientific). InstantBlue™ Protein Stain (Expedeon Ltd, UK) was used as a loading control. Amersham Hybond P 0.45 µm PVDF membranes (GE Healthcare, UK) were probed with the following antibodies (diluted 1:500 in either 5% (w/v) skimmed milk or 5% (w/v) BSA both in tris-buffered saline with 0.05% (v/v) Tween 20): mouse monoclonal anti-Alix<sup>25</sup>, rabbit polyclonal anti-CD63<sup>26</sup> (both purchased from Santa Cruz Biotechnology, USA); mouse monoclonal anti-CD81<sup>27</sup> (purchased from Bio-Rad, UK); rabbit monoclonal anti-Adiponectin<sup>28</sup> (purchased from Abcam, UK); rabbit monoclonal anti-CD9<sup>29</sup>, rabbit monoclonal anti-FABP4<sup>30</sup>; rabbit monoclonal anti-Perilipin<sup>31</sup> and rabbit monoclonal anti-PPARγ<sup>32</sup> (purchased from Cell Signaling Technologies, USA). Proteins were analysed using reducing conditions with the exception of the tetraspanins (CD9, CD63 and CD81), which were analysed using non-reducing conditions. Signals were detected using either goat anti-mouse IgG-HRP<sup>33</sup> or donkey anti-rabbit IgG-HRP<sup>34</sup> diluted 1:1000 in 5% (w/v) skimmed milk in tris-buffered saline with 0.05% (v/v) Tween 20) followed by Amersham ECL Western Blotting Detection Reagents (GE Healthcare).

## *Transmission Electron Microscopy*

Pooled EVs were resuspended in 1X 0.22 µm-filtered PBS and then fixed with an equal volume of 4% (v/v) paraformaldehyde and kept at 4°C until processing for TEM the next day. Briefly, EVs (10 µL) were adsorbed onto glow discharged carbon formvar 200 mesh copper grids for 2 minutes. Grids were then blotted using filter paper, stained for 10 seconds with 2% (w/v) uranyl acetate before surplus stain was removed and grids were air-dried. Grids were imaged using a FEI Tecnai 12 TEM at 120 kV fitted with a Gatan OneView CMOS camera.

*Sequential depletion of EV populations using magnetic beads*

Pooled EVs were diluted to a concentration of  $1 \times 10^{11}$  particles/mL using 1X 0.22  $\mu$ m-filtered PBS in replicates of three. EVs were then incubated for 2 hours at room temperature with 3  $\mu$ g/mL rabbit monoclonal anti-CD41 antibody<sup>35</sup> (purchased from Abcam). Fifty  $\mu$ L (per sample) of pre-washed Dynabeads™ M-280 sheep anti-rabbit IgG magnetic beads (Life Technologies, UK) were added to EVs/anti-CD41 and incubated with mixing for 30 minutes at room temperature. Samples were then introduced into the magnet (DynaMag™-2, Life Technologies) to deplete CD41+ EVs: this was quantified using NTA. The process was repeated sequentially with 3  $\mu$ g/mL rabbit monoclonal anti-CD11b<sup>36</sup>, rabbit polyclonal anti-CD144<sup>37</sup> and rabbit monoclonal anti-CD235a<sup>38</sup> antibodies (all purchased from Abcam) to deplete CD11b+, CD144+ and CD235a+ EVs. Final supernatants were quantified using NTA and analysed by Western Blot with “pre-depletion” samples for the presence of adipocyte and EV markers.

*Solid-phase-based depletion of EV populations*

High binding ELISA plates (Greiner Bio-One Ltd, UK) were coated in triplicate with rabbit monoclonal anti-CD41, -CD11b, -CD144 or -CD235a antibodies (Abcam, as above) diluted to 3  $\mu$ g/mL in PBS overnight at 4°C. Pooled EVs were diluted to a concentration of  $1 \times 10^{11}$  particles/mL as above and incubated for 2 hours at room temperature in wells containing anti-CD41 antibody to deplete CD41+ EVs. Supernatants were then transferred to wells containing anti-CD11b antibody for 2 hours at room temperature to deplete CD11b+ EVs. This process was then repeated sequentially with wells containing anti-CD144 antibody and anti-CD235a antibody to deplete CD144+ and CD235a+ EVs. Final supernatants were analysed as above.

*Time Resolved Fluorescence (TRF)*



The efficiency of depletion of major circulating EV populations was assessed using time resolved fluorescence (TRF) as previously described<sup>39,40</sup>. Briefly, EVs were normalised to a concentration of  $1 \times 10^{11}$  particles/mL in pre-depletion, post-CD41, post-CD11b, post-CD144 and post-CD235a samples from magnetic bead and solid phase-based depletion. EVs were then immobilised on high binding ELISA plates (Greiner Bio-One Ltd, UK) overnight at 4°C. EVs were blocked for 2 hours at room temperature using 1% (w/v) BSA before adding 3 µg/mL primary antibodies of interest (anti-CD41, anti-CD11b, anti-CD144 and anti-CD235a; as detailed above) in 0.1% (w/v) BSA overnight at 4°C. Primary antibodies were detected using a biotin-labeled goat anti-rabbit IgG secondary antibody<sup>41</sup> (diluted 1:2500 in 0.1% BSA, purchased from Perkin Elmer, UK) for 1 hour at room temperature, followed by a streptavidin-europium conjugate (diluted 1:1000 in red assay buffer, both Perkin Elmer) for 45 minutes at room temperature. Time resolved fluorescence was measured on a BMG CLARIOstar® plate reader (BMG Labtech, UK).

#### *Detection of an array of adipokines in plasma EV samples*

A commercially available Proteome Profiler Human Adipokine Array Kit (R&D Systems, Bio-Techne, UK) was used to analyse 58 adipocyte-related molecules in pre-depletion, post-magnetic bead depletion and post-solid phase depletion EV samples. Samples were diluted to load an absolute concentration of  $2 \times 10^{10}$  particles. The remainder of the experiment was performed according to the manufacturer's protocol. Dot assays were detected using Amersham ECL Hyperfilm following 15- and 60-minute exposures. Blots were scanned and pixel densities analysed using HLIimage++ (Western Vision Software, USA). A full list of analytes included in the kit is shown in Table S1.

#### *Statistical analysis*

182 Data are presented as mean  $\pm$  SEM. A one-way ANOVA with Tukey's Multiple Comparison Test was  
183 used to analyse the difference between means. A p value of  $<0.05$  was considered significant. Data  
184 were analysed using Graph Pad Prism (version 5; GraphPad Software Inc., CA).

185

## Results

### *Preparation of plasma-derived EVs using size exclusion chromatography*

Analysis of individual column fractions using Nanoparticle Tracking Analysis (NTA) showed a small peak in the concentration of particles/mL between fractions 5-10, followed by a large peak in particles and protein from fractions 12-26. Western blot analysis of fractions 2-28 showed the presence of both EV and adipocyte markers in fractions 6-10 but only adipocyte markers in fractions 11-28 (Figure S1). Plotting the ratio of particle concentration to protein concentration as described previously<sup>42</sup> showed fractions 5-10 to contain the highest number of particles:protein (Figure 1A). Therefore, these fractions were pooled and ultracentrifuged to pellet plasma-derived EVs. TEM of pelleted EVs indicated the presence of vesicle structures, and Western blot analysis showed the presence of classical EV and adipocyte markers in the pooled EVs of three different individuals (Figure 1B/C). Pooled EVs were shown to be deficient in the endoplasmic reticulum marker, Grp-94 (Figure S2A), in accordance with ISEV guidelines for expected proteins in EV isolates<sup>13</sup>. The supernatant of pelleted EVs following ultracentrifugation was deficient in CD9 (Figure S2B) indicating EVs were successfully pelleted by ultracentrifugation.

### *Adipocyte markers remain following sequential depletion of major EV families*

Magnetic beads and a solid phase-based method were used to sequentially deplete EVs bearing markers of the four major EV populations in the circulating plasma of three different individuals. TEM analysis revealed EV structures to be present in both post-magnetic bead and post-solid phase depletion samples (Figure 2A). EV concentration was reduced by ~75% in both post-magnetic bead and post-solid phase depletion samples:  $1.01 \times 10^{11} \pm 1.00 \times 10^{10}$  particles/mL to  $3.10 \times 10^{10} \pm 6.90 \times 10^9$  particles/mL and  $2.50 \times 10^{10} \pm 6.50 \times 10^9$  particles/mL respectively,  $p < 0.001$ , (n=5); Figure 2B. The detection of markers of the main EV populations in plasma (Platelet; CD41, monocytes; CD11b, endothelial cells; CD144 and erythrocytes; CD235a) were reduced in post-depletion samples following magnetic bead and solid-phase-based methods (Figure S3). Adiponectin, FABP4, PPAR $\gamma$ ,

Perilipin, CD9 and Alix were reduced but still detectable in post-magnetic bead and post-solid phase depletion samples (Figure 2C). Interestingly, only the adipocyte specific PPAR $\gamma$ -2 isoform remained in post-depletion samples.

#### *Major adipokines are expressed in pre and post-depletion samples*

An adipokine array kit was used to probe for 58 adipokines (Table S1) in pre-depletion, post-magnetic bead and post-solid phase depletion plasma EV samples (Figure 3A). Major adipokines, including adiponectin, adipsin, leptin, preadipocyte factor (PREF)-1, resistin and visfatin, were detected in all samples (Figure 3B). No significant differences were observed between samples.

## Discussion

This study is the first of its kind to present a variety of evidence for the presence of adipocyte-derived EVs in the circulating plasma of healthy individuals. A panel of adipocyte markers and adipokines were detected in plasma EV samples after careful sample processing and depletion of EVs from major circulating sources. Adipocyte-derived EVs have proven to be important, novel endocrine mediators of adipocytes *in vitro*, thus their detection in the human circulation is an important step towards understanding their roles as mediators of adipocyte function, including potential effects on vascular health.

Due to the complexity of plasma as a biofluid, platelet-depleted plasma was loaded onto size exclusion chromatography (SEC) columns. SEC has previously been shown to separate EVs quickly and effectively from the majority of non-vesicular protein in plasma<sup>39,43</sup>. Here, EVs were identified in fractions 5-10 from the high particle-to-protein ratio and the presence of EV markers, CD9, CD81 and Alix in these fractions (Figure 1 and Figure S1). Later fractions had a low particle-to-protein ratio and EV markers were not identified in these fractions. Additionally, the adipocyte markers adiponectin, FABP4, Perilipin and PPAR $\gamma$  were detected in fractions 5-10 but were also present in later fractions. Detection of these markers is in keeping with previous studies that have identified adipocyte markers within EVs from human plasma<sup>4,11,18,22</sup>. However, our data indicates that markers previously used to identify adipocyte-derived EVs in un-purified plasma samples are largely soluble and likely not associated with EVs as illustrated in Figure S1, where we show adiponectin, FABP4, Perilipin and PPAR $\gamma$  are all detected as soluble protein in SEC fractions not containing EVs, despite loading up to 55x less volume. This finding has important implications for the measurement of adipocyte EV markers in human plasma, and highlights the importance of techniques such as SEC prior to analysis of adipocyte markers to avoid erroneous overestimations from soluble material. Pooling and subsequent ultracentrifugation of these fractions confirmed the presence of EV structures by TEM and both EV and adipocyte proteins by Western blotting (Figure 1, Figure S2A/B). We also observed the presence of adipokines in the supernatant of pelleted EVs highlighting the importance of the ultracentrifugation step after SEC. This is in keeping with previous studies, which have shown that

SEC is effective in removing ~95% of non-vesicular protein in a single step, but the EV-free supernatant is likely to contain residual, non-EV-associated plasma proteins, including adipokines<sup>39,43</sup>. The majority of plasma-derived EVs originate from cells that are in direct contact with blood, such as platelets, leukocytes, vascular endothelial cells and erythrocytes<sup>44</sup>. The location of adipocytes within adipose tissue may hinder the majority of adipocyte-derived EVs reaching the systemic circulation. Consequently, adipocyte-derived EVs are likely to form only a minor proportion of plasma-derived EVs. Furthermore, markers that uniquely identify adipocytes, such as adiponectin are readily secreted. High-speed centrifugation used for EV isolation may co-pellet these soluble markers with EVs, lending a false adipocyte character. We therefore applied two separate techniques to deplete the major circulating populations of plasma-derived EVs to establish whether adipocyte markers were reduced by depletion of “non-adipocyte” EVs and whether an adipocyte protein signature was retained post-depletion. EV structures were visible by TEM following sequential depletion of major plasma EV populations (Figure 2A) though the overall concentration of EVs detected by NTA was reduced by around 75% (Figure 2B). Both techniques were shown to reduce the expression of each marker used for depletion, with the magnetic bead based approach depleting these markers beyond detection by time resolved fluorescence (Figure S3). This suggests both techniques are effective in reducing the populations of major circulating EVs in plasma. Expression of adiponectin, FABP4 and PPAR $\gamma$  was reduced post-depletion (Figure 2C), suggesting a proportion of these markers are in some way associated with EVs from non-adipocyte populations. Although their expression is predominantly associated with adipocytes, both FABP4 and PPAR $\gamma$  have previously been shown to be produced by other cells including macrophages<sup>45,46</sup> perhaps explaining the partial loss in signal post-depletion. FABP4 was not detected in all samples (possibly due to individual variations in donors) and was often detected at a higher molecular weight than expected. FABP4 has previously been reported to form homodimers, particularly upon ligand activation<sup>47</sup> though the absence of expression in some samples reaffirms the need to use multiple markers when analysing adipocyte-derived EVs. However, whilst both isoforms of PPAR $\gamma$  were detected in pre-depletion samples, only PPAR $\gamma$ 2 remained in post-depletion samples. PPAR $\gamma$ 2 is an adipocyte-specific nuclear transcription factor<sup>48</sup> and its presence in

combination with adiponectin, FABP4 and Perilipin in post-depletion samples is highly indicative of adipocyte origin. Furthermore, a number of major adipokines were detected in post-depletion samples using an adipokine array kit, including the angiogenic factors leptin and resistin, and adipokines adipsin, PREF-1, and visfatin (Figure 3). This further evidences the presence of adipocyte markers in EV samples that have been depleted of major circulating plasma EV populations. The EV markers Alix and CD9 were reduced but still present in post-depletion samples (Figure 2C). This tallies with a reduced concentration of EVs but also indicates that EVs are still present in post-depletion samples, supporting the TEM data. Taken together, our data show that after depleting EVs from major sources in plasma using either magnetic beads or solid phase depletion, adipocyte and EV markers are still detectable, supporting the presence of adipocyte-derived EVs. It is important to note that we observed differences in expression patterns of both EV and adipocyte markers between individuals, however, this is most likely due to natural biological variation within our small group of donors.

In conclusion, this study is the first of its kind to provide evidence for the presence of adipocyte-derived EVs in circulating plasma using multiple adipocyte and EV markers, and conducted in accordance with international recommendations. Our data also emphasize the need for careful EV preparation when analysing adipocyte markers to avoid contribution of signal from soluble adipocyte material. Whilst adipocyte-derived EVs may only constitute a relatively small fraction of the total EV population in circulating plasma, this may not necessarily reflect a minor effect on vascular health since the content of the EVs is likely to dictate their function, particularly in EVs derived from dysfunctional adipocytes. Our data thus provide a platform for future investigations into circulating adipocyte-derived EVs as potential novel biomarkers of adipocytes in health and obesity-driven cardiovascular disease.

## **Acknowledgements**

The authors would like to thank Dr. Justyna Witczak and Mrs. Margaret Munnery for the phlebotomy required for this work. We would also like to thank the healthy individuals who volunteered for the study and the Dunn School EM facility for the TEM analyses.

## References

1. Trayhurn P, Wood IS. Adipokines: inflammation and the pleiotropic role of white adipose tissue. *Br J Nutr.* 2004;92(3):347-355.
2. Wang B, Wood IS, Trayhurn P. Dysregulation of the expression and secretion of inflammation-related adipokines by hypoxia in human adipocytes. *Pflugers Arch.* 2007;455(3):479-492.
3. Kralisch S, Ebert T, Lossner U, Jessnitzer B, Stumvoll M, Fasshauer M. Adipocyte fatty acid-binding protein is released from adipocytes by a non-conventional mechanism. *Int J Obes (Lond).* December 2013.
4. Kranendonk MEG, Visseren FLJ, van Balkom BWM, Nolte-'t Hoen ENM, van Herwaarden JA, de Jager W, Schipper HS, Brenkman AB, Verhaar MC, Wauben MHM, Kalkhoven E. Human adipocyte extracellular vesicles in reciprocal signaling between adipocytes and macrophages. *Obesity (Silver Spring).* 2014;22(5):1296-1308.
5. Kranendonk MEG, Visseren FLJ, van Herwaarden JA, Nolte-'t Hoen ENM, de Jager W, Wauben MHM, Kalkhoven E. Effect of extracellular vesicles of human adipose tissue on insulin signaling in liver and muscle cells. *Obesity (Silver Spring).* 2014;22(10):2216-2223.
6. Connolly KD, Guschina IA, Yeung V, Clayton A, Draman MS, Ruhland C Von, Ludgate M, James PE, Rees DA. Characterisation of adipocyte-derived extracellular vesicles released pre- and post-adipogenesis. *J Extracell Vesicles.* 2015;4.
7. DeClercq V, d'Eon B, McLeod RS. Fatty acids increase adiponectin secretion through both classical and exosome pathways. *Biochim Biophys Acta.* 2015;1851(9):1123-1133.
8. Eguchi A, Mulya A, Lazic M, Radhakrishnan D, Berk MP, Povero D, Gornicka A, Feldstein AE. Microparticles release by adipocytes act as “find-me” signals to promote macrophage migration. *PLoS One.* 2015;10(4):e0123110.



- 326 9. Ertunc ME, Sikkeland J, Fenaroli F, Griffiths G, Daniels MP, Cao H, Saatcioglu F,  
327 Hotamisligil GS. Secretion of fatty acid binding protein aP2 from adipocytes through a  
328 nonclassical pathway in response to adipocyte lipase activity. *J Lipid Res.* 2015;56(2):423-434.
- 329 10. Ferrante SC, Nadler EP, Pillai DK, Hubal MJ, Wang Z, Wang JM, Gordish-Dressman H,  
330 Koeck E, Sevilla S, Wiles AA, Freishtat RJ. Adipocyte-derived exosomal miRNAs: a novel  
331 mechanism for obesity-related disease. *Pediatr Res.* 2015;77(3):447-454.
- 332 11. Eguchi A, Lazic M, Armando AM, Phillips SA, Katebian R, Maraka S, Quehenberger O, Sears  
333 DD, Feldstein AE. Circulating adipocyte-derived extracellular vesicles are novel markers of  
334 metabolic stress. *J Mol Med.* 2016;94(11):1241-1253.
- 335 12. Durcin M, Fleury A, Taillebois E, Hilairat G, Krupova Z, Henry C, Truchet S, Trötz Müller M,  
336 Köfeler H, Mabilieu G, Hue O, Andriantsitohaina R, Martin P, Le Lay S. Characterisation of  
337 adipocyte-derived extracellular vesicle subtypes identifies distinct protein and lipid signatures  
338 for large and small extracellular vesicles. *J Extracell Vesicles.* 2017;6(1):1305677.
- 339 13. Lötval J, Hill AF, Hochberg F, Buzás EI, Di Vizio D, Gardiner C, Gho YS, Kurochkin I V,  
340 Mathivanan S, Quesenberry P, Sahoo S, Tahara H, Wauben MH, Witwer KW, Théry C.  
341 Minimal experimental requirements for definition of extracellular vesicles and their functions:  
342 a position statement from the International Society for Extracellular Vesicles. *J Extracell*  
343 *vesicles.* 2014;3:26913.
- 344 14. Müller G, Jung C, Straub J, Wied S, Kramer W. Induced release of membrane vesicles from  
345 rat adipocytes containing glycosylphosphatidylinositol-anchored microdomain and lipid  
346 droplet signalling proteins. *Cell Signal.* 2009;21(2):324-338.
- 347 15. Han Y, Bai Y, Yan X, Ren J, Zeng Q, Li X, Pei X, Han Y. Co-transplantation of exosomes  
348 derived from hypoxia-preconditioned adipose mesenchymal stem cells promotes  
349 neovascularization and graft survival in fat grafting. *Biochem Biophys Res Commun.*  
350 2018;497(1):305-312.

16. Kang T, Jones TM, Naddell C, Bacanamwo M, Calvert JW, Thompson WE, Bond VC, Chen YE, Liu D. Adipose-Derived Stem Cells Induce Angiogenesis via Microvesicle Transport of miRNA-31. *Stem Cells Transl Med.* 2016;5(4):440-450.
17. Berckmans RJ, Nieuwland R, Böing AN, Romijn FP, Hack CE, Sturk A. Cell-derived microparticles circulate in healthy humans and support low grade thrombin generation. *Thromb Haemost.* 2001;85(4):639-646.
18. Gustafson CM, Shepherd AJ, Miller VM, Jayachandran M. Age- and sex-specific differences in blood-borne microvesicles from apparently healthy humans. *Biol Sex Differ.* 2015;6:10.
19. Arraud N, Linares R, Tan S, Gounou C, Pasquet J-M, Mornet S, Brisson AR. Extracellular vesicles from blood plasma: determination of their morphology, size, phenotype and concentration. *J Thromb Haemost.* 2014;12(5):614-627.
20. Phoonsawat W, Aoki-Yoshida A, Tsuruta T, Sonoyama K. Adiponectin is partially associated with exosomes in mouse serum. *Biochem Biophys Res Commun.* 2014;448(3):261-266.
21. van der Pol E, Hoekstra AG, Sturk A, Otto C, van Leeuwen TG, Nieuwland R. Optical and non-optical methods for detection and characterization of microparticles and exosomes. *J Thromb Haemost.* 2010;8(12):2596-2607.
22. Looze C, Yui D, Leung L, Ingham M, Kaler M, Yao X, Wu WW, Shen R-F, Daniels MP, Levine SJ. Proteomic profiling of human plasma exosomes identifies PPARgamma as an exosome-associated protein. *Biochem Biophys Res Commun.* 2009;378(3):433-438.
23. Shah MD, Bergeron AL, Dong J-F, López JA. Flow cytometric measurement of microparticles: pitfalls and protocol modifications. *Platelets.* 2008;19(5):365-372.
24. Witwer KW, Buzás EI, Bemis LT, Bora A, Lässer C, Lötvall J, Nolte-'t Hoen EN, Piper MG, Sivaraman S, Skog J, Théry C, Wauben MH, Hochberg F. Standardization of sample collection, isolation and analysis methods in extracellular vesicle research. *J Extracell vesicles.*

375 2013;2.

376 25. RRID: AB\_10608844.

377 26. RRID: AB\_648179.

378 27. RRID: AB\_323286.

379 28. RRID: AB\_1523093.

380 29. RRID: AB\_2732848.

381 30. RRID: AB\_2278527.

382 31. RRID: AB\_10829911.

383 32. RRID: AB\_10694772.

384 33. RRID: AB\_650499.

385 34. RRID: AB\_2722659.

386 35. RRID: AB\_2732852.

387 36. RRID: AB\_868788.

388 37. RRID: AB\_870662.

389 38. RRID: AB\_2732853.

390 39. Welton JL, Webber JP, Botos L-A, Jones M, Clayton A. Ready-made chromatography  
391 columns for extracellular vesicle isolation from plasma. *J Extracell vesicles*. 2015;4:27269.

392 40. Burnley-Hall N, Abdul F, Androshchuk V, Morris K, Ossei-Gerning N, Anderson R, Rees D,  
393 James P. Dietary Nitrate Supplementation Reduces Circulating Platelet-Derived Extracellular  
394 Vesicles in Coronary Artery Disease Patients on Clopidogrel Therapy: A Randomised,  
395 Double-Blind, Placebo-Controlled Study. *Thromb Haemost*. 2018;118(01):112-122.

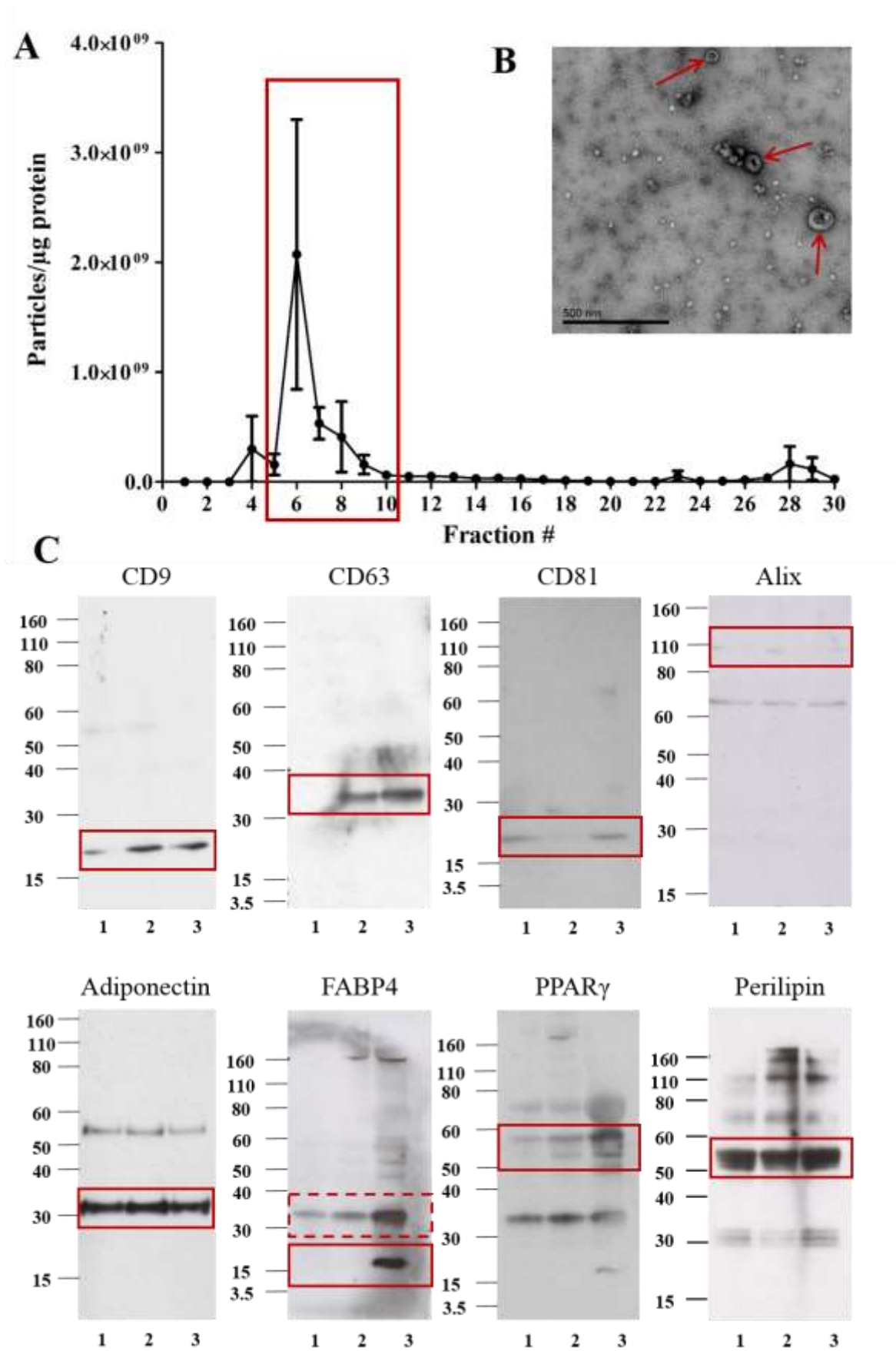
- 396 41. RRID: AB\_2732854.
- 397 42. Webber J, Clayton A. How pure are your vesicles? *J Extracell vesicles*. 2013;2.
- 398 43. Böing AN, van der Pol E, Grootemaat AE, Coumans FAW, Sturk A, Nieuwland R. Single-step  
399 isolation of extracellular vesicles by size-exclusion chromatography. *J Extracell vesicles*.  
400 2014;3.
- 401 44. Christersson C, Johnell M, Siegbahn A. Evaluation of microparticles in whole blood by  
402 multicolour flow cytometry assay. *Scand J Clin Lab Invest*. 2013;73(3):229-239.
- 403 45. Makowski L, Boord JB, Maeda K, Babaev VR, Uysal KT, Morgan MA, Parker RA, Suttles J,  
404 Fazio S, Hotamisligil GS, Linton MF. Lack of macrophage fatty-acid-binding protein aP2  
405 protects mice deficient in apolipoprotein E against atherosclerosis. *Nat Med*. 2001;7(6):699-  
406 705.
- 407 46. Rosen ED, Sarraf P, Troy AE, Bradwin G, Moore K, Milstone DS, Spiegelman BM,  
408 Mortensen RM. PPAR gamma is required for the differentiation of adipose tissue in vivo and  
409 in vitro. *Mol Cell*. 1999;4(4):611-617.
- 410 47. Gillilan RE, Ayers SD, Noy N. Structural Basis for Activation of Fatty Acid-binding Protein 4.  
411 *J Mol Biol*. 2007;372(5):1246-1260.
- 412 48. Tontonoz P, Hu E, Devine J, Beale EG, Spiegelman BM. PPAR gamma 2 regulates adipose  
413 expression of the phosphoenolpyruvate carboxykinase gene. *Mol Cell Biol*. 1995;15(1):351-  
414 357.

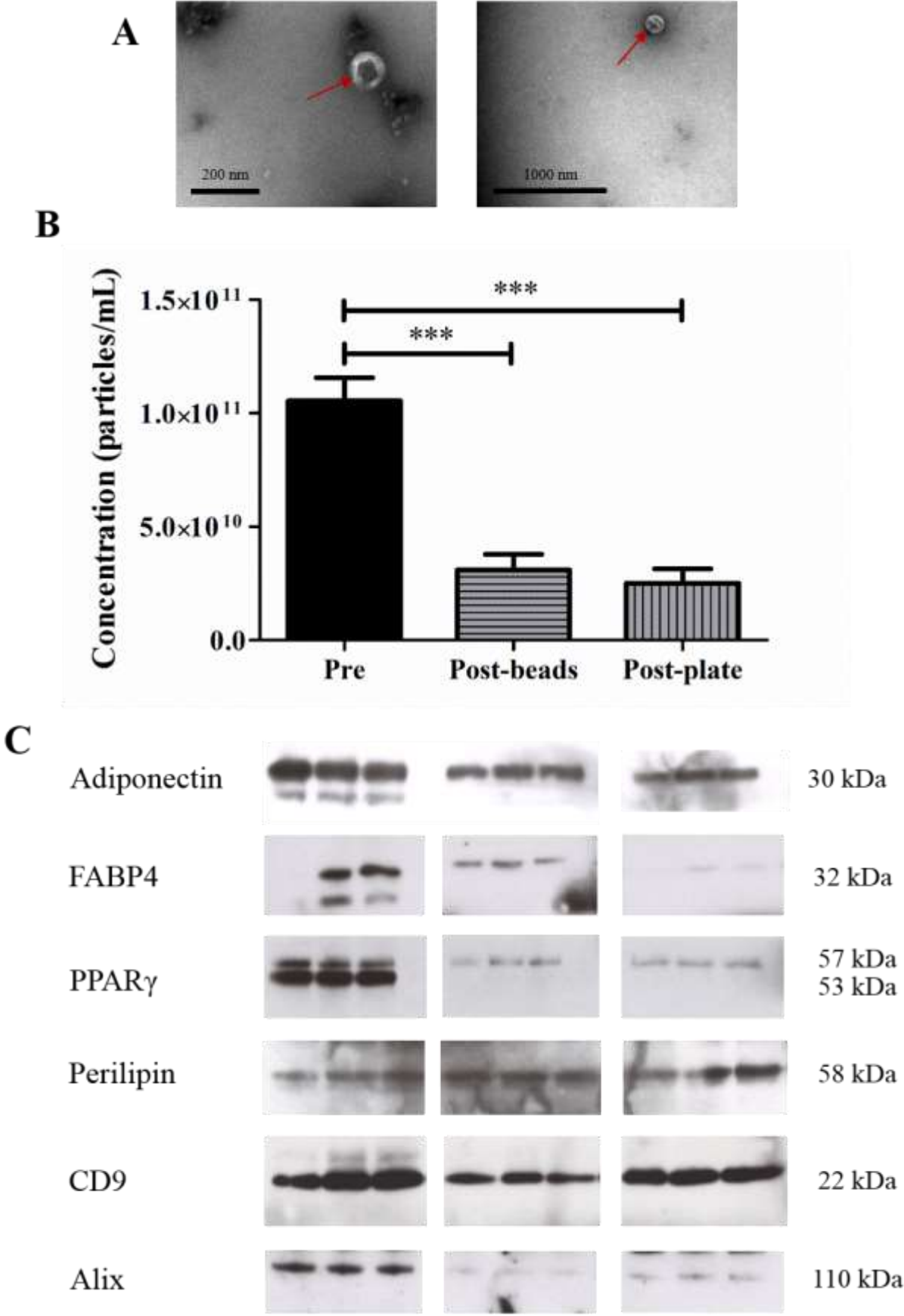
415

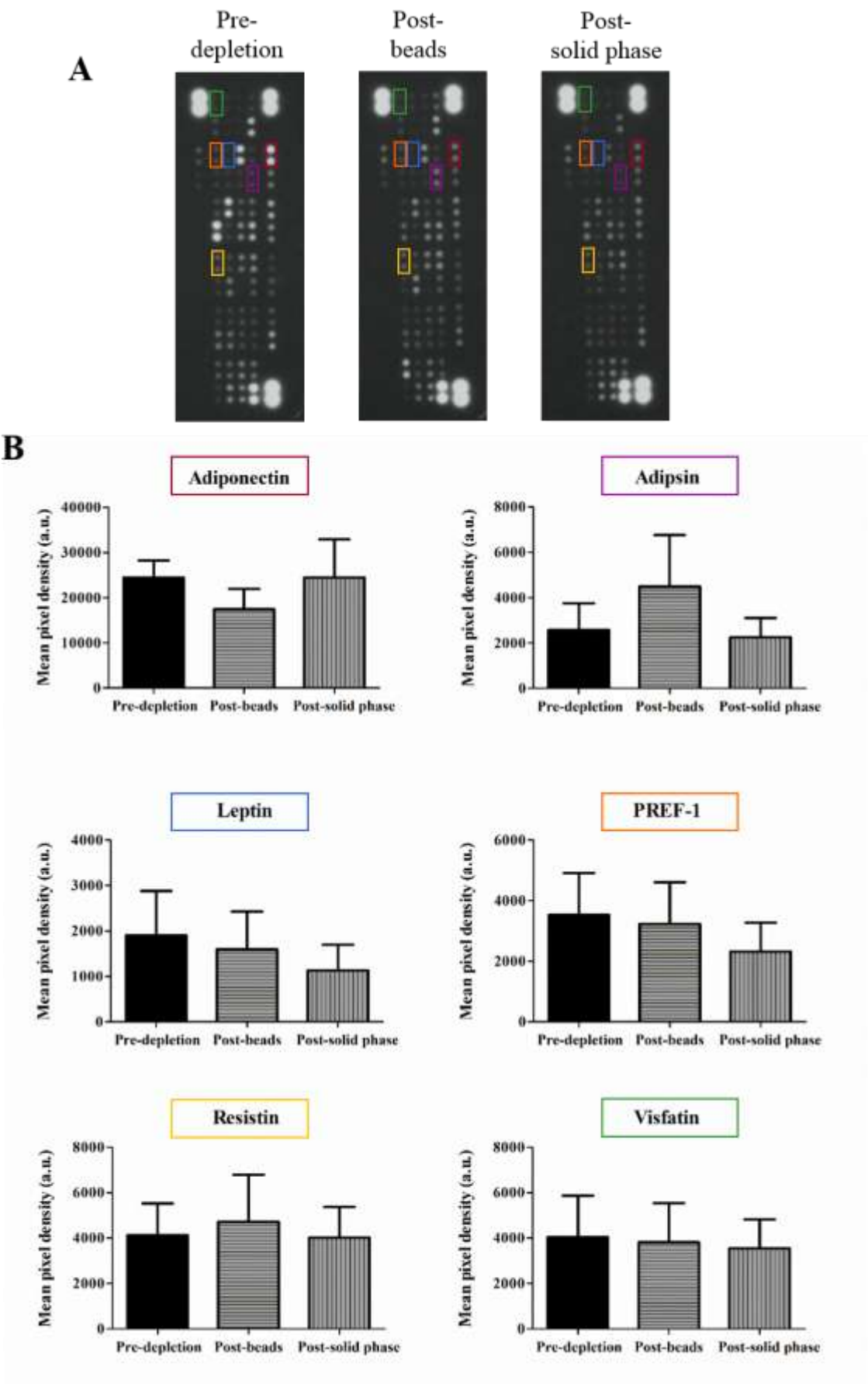
**Figure 1: Detailed analysis of pooled plasma EVs.** (A) Fractions 5-10 showed the highest ratio of particles-to-protein and the presence of EV structures by TEM (B, red arrows indicate EV structures) following ultracentrifugation. (C) Pooled EVs from three different individuals (labelled 1, 2, and 3) were analysed by Western blot for EV markers: CD9, CD63, CD81 and Alix, and adipocyte markers: Adiponectin, FABP4, PPAR $\gamma$  and Perilipin (n=3). Solid red boxes indicate the predicted molecular weight for each antigen; the dotted red box may indicate a FABP4 dimer ~32 kDa.

**Figure 2: Adipocyte and EV markers were maintained post-magnetic bead and solid phase depletion.** (A) EV structures were visible by TEM in post-magnetic bead depletion (left, scale bar 200 nm) and post-solid phase depletion (right, scale bar 1000 nm). (B) EV concentration was reduced following sequential depletion of major EV families using magnetic beads or a solid phase method, \*\*\* $p = 0.005$  (n=5). (C) Adiponectin, FABP4, PPAR $\gamma$ -2, Perilipin, CD9 and Alix were still present in post-depletion samples of three different individuals.

**Figure 3: Major adipokines were present in post-magnetic bead and –solid phase depletion samples.** (A) Inverted raw data of dot blots pre-depletion, post-magnetic beads and post-solid phase depletion. Major adipokines are highlighted with corresponding pixel densities (B). Representative dot blots of n=3.









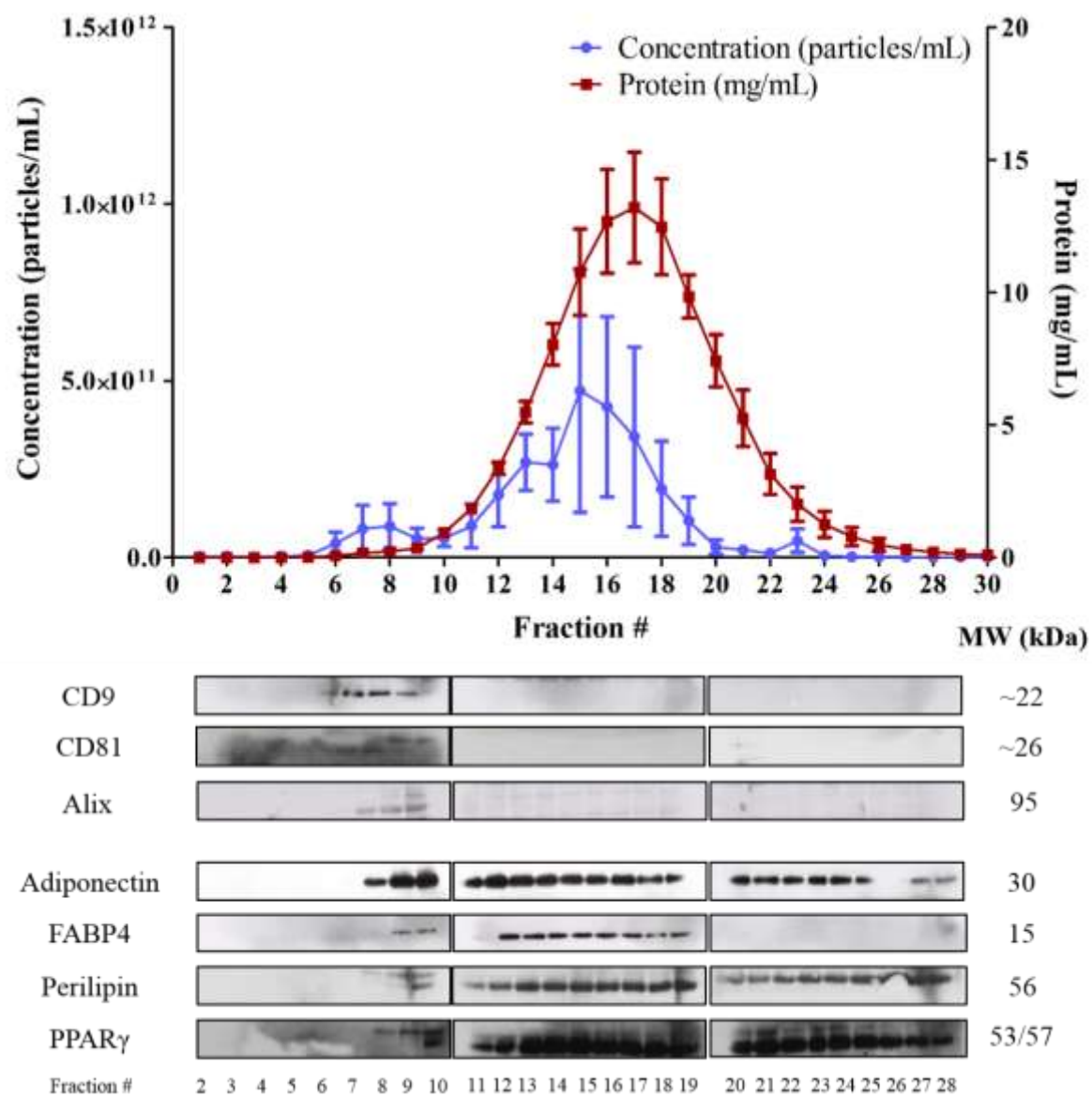
## Supplemental data

**Figure S1: Co-elution of EV and adipocyte markers from human plasma.** Plasma (1 mL) was loaded onto SEC columns and 30 x 500  $\mu$ L fractions were collected. The concentration of particles/mL was measured using NTA and the protein concentration was measured using Nanodrop for each fraction. Fractions 2 – 28 were then analysed by Western blot (8  $\mu$ g/lane) for the EV markers; CD9, CD81 and Alix, and the adipocyte markers; Adiponectin, FABP4, Perilipin and PPAR $\gamma$ . A small peak in particle concentration in fractions 5-10 corresponds with the detection of EV and adipocyte markers. A larger peak in particles and protein in fractions 12-26 corresponds with adipocyte markers only (n=3).

**Figure S2: Confirmation of an EV population.** (A) Western blot analysis of 3T3-L1 cell (positive control to confirm antibody specificity) and pooled plasma EV lysates for the endoplasmic reticulum protein, Grp-94 (MW~100 kDa). (B) Western blot analysis of pooled plasma EVs and the corresponding supernatant from the EV pellet following ultracentrifugation for the EV marker, CD9 (MW~ 22kDa).

**Figure S3: The efficiency of magnetic bead and solid phase depletion.** Equal numbers of EVs were immobilised onto ELISA plates pre- and post-CD41, -CD11b, -CD144 and -CD235a depletion using magnetic beads (A) and solid phase (B). Pre and post samples were then analysed by time resolved fluorescence for the presence of the depleted marker and plotted as a percentage of the “Pre” sample fluorescence. ND = not detected.

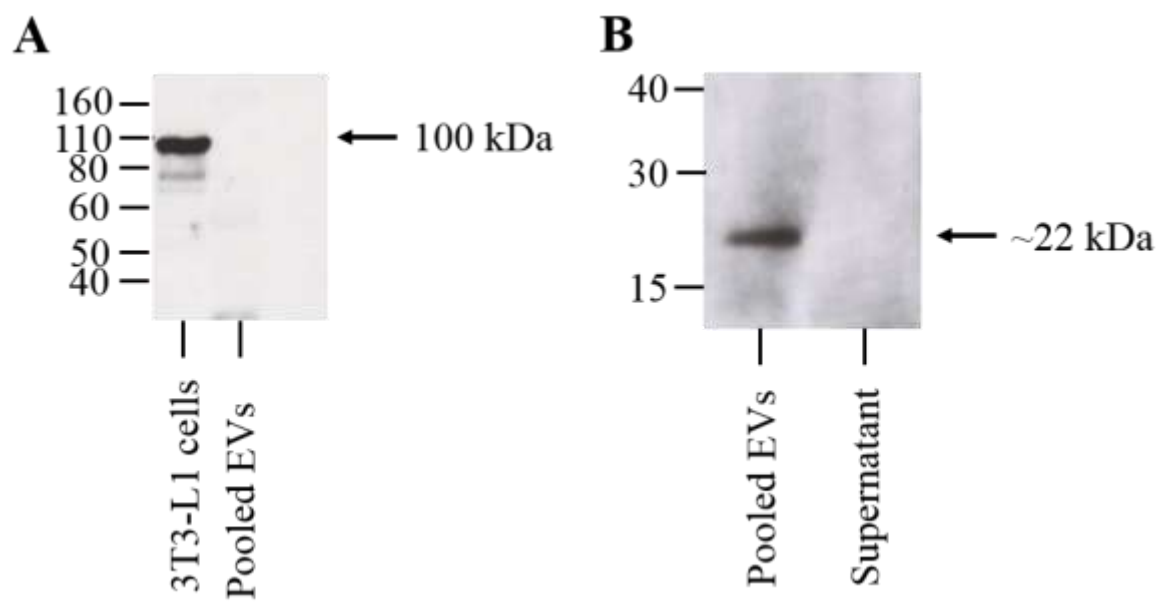
**Table S1: Adipokine array appendix.** A list of the 58 analytes included in adipokine array kit with mean pixel density values  $\pm$  SEM for pre-depletion, post-magnetic bead depletion and post-solid phase depletion samples (n=3).



463

464

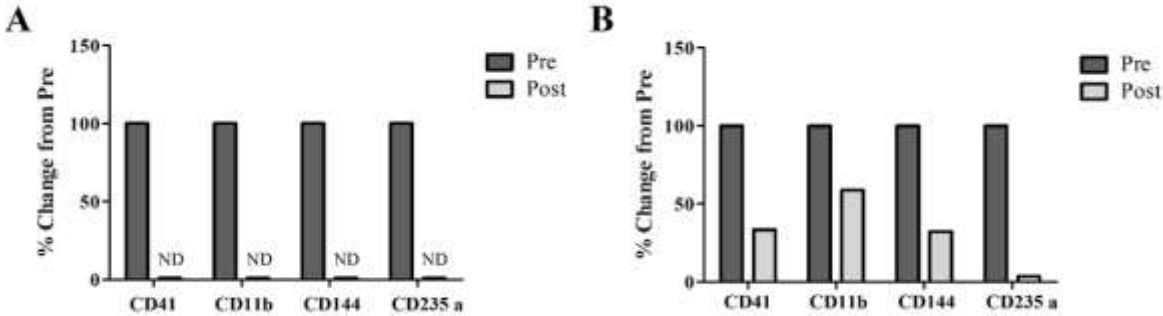
465 **Supplementary Figure 2**



466

467

468      **Supplementary Figure 3**



469

470

471 **Supplementary Table 1**

<b>Adipokine</b>	<b>Pre-depletion</b>	<b>Post-beads</b>	<b>Post-solid phase</b>
Adiponectin	24,425 ± 3,808	17,417 ± 4,531	24, 429 ± 8,412
Angiopoietin-1	5,978 ± 2,030	4,961 ± 1,892	5,465 ± 2,071
Angiopoietin-2	9,963 ± 2,596	8,095 ± 2,270	7,482 ± 2,509
Angiopoietin-like 2	7,484 ± 1,997	6,260 ± 2,090	5,543 ± 2,023
Angiopoietin-like 3	2,153 ± 908	2,582 ± 1,075	1,772 ± 721
CD257 (B cell activating factor)	3,182 ± 1,165	3,212 ± 1,280	2,584 ± 933
Bone morphogenetic protein (BMP)-4	3,403 ± 1,269	3,267 ± 1,392	3,565 ± 1,212
Cathepsin D	8,320 ± 2,891	7,734 ± 3,011	11,028 ± 5,763
Cathepsin L	3,310 ± 1,690	9,065 ± 3,214	2,661 ± 1,404
Cathepsin S	13,899 ± 4,093	13,172 ± 4,106	11,031 ± 4,783
Chemerin	2,000 ± 983	2,405 ± 1,119	1,964 ± 790
Complement Factor D (Adipsin)	2,578 ± 1,173	4,494 ± 2,262	2,254 ± 851
C-Reactive Protein (CRP)	8,585 ± 3,518	6,317 ± 1,873	8,281 ± 3,709
Dipeptidyl peptidase (DPP)-4	9,591 ± 3,337	11,138 ± 3,757	10,306 ± 4,681
Endocan	7,882 ± 2,761	9,140 ± 3,097	7,221 ± 2,227
EN-RAGE	3,846 ± 1,619	4,634 ± 1,763	3,033 ± 1,110
Fetuin B	2,620 ± 964	3,060 ± 1,265	2,104 ± 659
Fibroblast Growth Factor (FGF)-2	2,407 ± 921	2,355 ± 1,156	1,624 ± 426
FGF-19	6,987 ± 2,361	5,403 ± 2,117	7,197 ± 2,920
Fibrinogen	35,002 ± 4,995	38,828 ± 2,134	36,146 ± 5,145
Growth Hormone	2,314 ± 571	3,279 ± 738	2,149 ± 62
Hepatocyte growth factor (HGF)	1,932 ± 382	2,340 ± 402	1,210 ± 604
Intercellular adhesion molecule (ICAM)-1	11,422 ± 5,785	8,230 ± 1,496	7,768 ± 1,746
Insulin growth factor binding protein (IGFBP)-2	3,047 ± 290	2,243 ± 881	1,313 ± 603
IGFBP-3	4,233 ± 1,710	3,945 ± 1,320	3,489 ± 1,225

IGFBP-4	7,911 ± 2,475	8,848 ± 3,219	6,903 ± 2,286
IGFBP-6	5,850 ± 2,075	7,141 ± 2,633	5,144 ± 1,663
IGFBP-7	1,206 ± 185	1,451 ± 20	527 ± 398
Interleukin (IL)-1 $\beta$	2,921 ± 930	3,149 ± 1,269	2,447 ± 891
IL-6	3,234 ± 1,039	3,238 ± 1,417	2,919 ± 1,260
IL-8	7,350 ± 2,172	7,811 ± 2,729	8,001 ± 3,149
IL-10	8,716 ± 3,176	8,237 ± 3,133	10,025 ± 3,603
IL-11	1,928 ± 892	2,622 ± 1,351	1,779 ± 823
Transforming growth factor (TGF)- $\beta$ 1	1,687 ± 282	2,024 ± 327	1,601 ± 34
Leptin	1,902 ± 978	1,596 ± 832	1,135 ± 567
Leukaemia inhibitory factor (LIF)	2,310 ± 1,056	2,055 ± 906	1,704 ± 748
Lipocalin-2	26,197 ± 2,855	24,184 ± 7,044	24,200 ± 8,432
Monocyte chemoattractant protein (MCP)-1	2,640 ± 676	2,864 ± 1,047	2,464 ± 430
Macrophage colony stimulating factor (M-CSF)	2,847 ± 1,034	3,270 ± 1,435	2,161 ± 709
Macrophage migration inhibitory factor (MIF)	4,646 ± 1,785	12,566 ± 2,293	4,130 ± 1,121
Myeloperoxidase	2,035 ± 641	2,378 ± 1,054	1,727 ± 503
Nidogen-1	4,820 ± 1,340	7,034 ± 2,488	4,173 ± 1,853
Oncostatin M	4,984 ± 1,743	3,647 ± 1,555	4,961 ± 2,042
Pappalysin-1	8,222 ± 2,764	5,699 ± 2,099	8,715 ± 3,445
Pentraxin-3	3,903 ± 1,809	3,639 ± 1,703	3,401 ± 1,608
Preadipocyte factor (PREF)-1	3,525 ± 1,393	3,237 ± 1,378	2,325 ± 943
Proprotein convertase 9	1,953 ± 937	1,904 ± 969	1,423 ± 706
RAGE	3,676 ± 663	3,041 ± 1,251	3,194 ± 1,202
CCL5	26495 ± 6,371	15,406 ± 4,790	25,518 ± 8,363
Resistin	4,121 ± 2,436	4,731 ± 2,062	4,024 ± 1,348
Serpin A8	1,712 ± 639	1,979 ± 826	1,437 ± 499
Serpin A12	2,215 ± 128	1,997 ± 990	1,327 ± 329

Plasminogen activator inhibitor (PAI)-1	5,613 ± 1,623	4,858 ± 1,909	4,560 ± 1,853
Tissue inhibitor of metalloproteinase (TIMP)-1	4,024 ± 1,006	24,028 ± 4,264	3,550 ± 1,231
TIMP-3	1,932 ± 390	1,015 ± 352	1,557 ± 690
Tumor necrosis factor (TNF)- $\alpha$	4,260 ± 1,574	5,900 ± 2,245	4,942 ± 1,872
Vascular endothelial growth factor (VEGF)	2,338 ± 160	2,669 ± 1,105	1,555 ± 716
Visfatin	4,029 ± 1,842	3,820 ± 1,715	3,540 ± 1,285

472

473